J. LINDHARD, VIBEKE NIELSEN AND M. SCHARFF(†)

APPROXIMATION METHOD IN CLASSICAL SCATTERING BY SCREENED COULOMB FIELDS

(Notes on Atomic Collisions, I)

Det Kongelige Danske Videnskabernes Selskab
Matematisk-fysiske Meddelelser **36**, 10

Kommissionær: Munksgaard
København 1968

CONTENTS

Synopsis

The paper presents a comprehensive approximation formula for classical scattering of fast ions by atoms. The formula has been applied in previous papers.

We discuss at first the simplifications and the errors resulting from the use of a Thomas-Fermi type potential in scattering calculations. The accuracy of classical mechanics in such scattering problems is treated briefly.

We study scattering by power law potentials for low angle deflections and derive a wide angle extrapolation in terms of a one-parameter formula. The formula is applied to Thomas-Fermi potentials, where the reduced scattering cross section is found numerically as a function of a single scattering parameter. The stopping cross section is obtained as a function of reduced energy. We derive the magic formula, which leads to easy estimates of scattering in any potential, and compare scattering by several types of screened potentials. Comparison is also made with more precise computations of scattering.

PRINTED IN DENMARK
BIANCO LUNOS BOGTRYKKERI A/S

§ 1. Introduction

The present paper is subtitled "Notes on Atomic Collisions, I", and belongs to a group of four papers. Although the publication of the paper has been delayed, some of its results were quoted and utilized in a summarizing article[11] and in the already published Notes II[12] and III[13], as well as in other associated papers[14, 15, 16, 17]. In point of fact, the essential parts of the paper were worked out in the years 1958–59 as a necessary basis for our studies of slowing-down of heavy ions. At that time, little was known about details of the collisions in question, but during later years experimental and theoretical results have improved the knowledge in this field. Nevertheless, we adhere to the original treatment. The reason for doing this is partly that we want to state the precise basis of the formulae used in later work, and partly that attempts at improvement of the general framework would hardly be physically justified at present.

The main point in this paper, as in Notes IV (unpublished), is that collisions between ions and atoms may be described approximately in terms of similarity properties, where, at first, merely one parameter suffices to embrace all scattering processes. In Notes II and III, these extremely simple similarity properties are found to lead to significant simplifications in the theory of particle radiation effects.

More definitely, the purpose of the paper is to find comprehensive approximation methods for treating elastic scattering of ions by atoms. The scattering problem is comparatively simple since we disregard the inelastic effects, which are studied in Notes IV. In the following, we shall therefore mainly discuss approximation methods from a formal point of view, with less emphasis on their physical justification or on their application to studies of ranges and radiation damage. It may be appropriate, however, to sketch at first the background for the introduction of the present scattering method. This is done in § 2, where we consider the various approximations involved in the use of a simple interaction potential in scattering calculations. The magnitude of the potential is also discussed, and we consider briefly the

justification for the use of classical mechanics in ion-atom scattering. After this preamble, we study in § 3 scattering by power law potentials, and find that low angle deflections may be extrapolated to wide angles in terms of a one-parameter formula, retaining a fair accuracy. This treatment is applied to Thomas-Fermi type potentials in § 4, where the reduced scattering cross section is given as a function of a single scattering parameter. In § 5 we derive the magic formula which leads to easy estimates of scattering in any potential, and we compare scattering by several types of screened potentials. The present scaling formulae are compared with more precise scattering calculations.

§ 2. General Considerations

Ion-Atom Collisions at Low Velocities

Consider an ion, with charge number Z_1 and velocity v, colliding with an atom at rest with charge number Z_2. We disregard excitations and ejection of electrons from ion or atom during the collision. Although such inelastic effects are important in many respects, they may in first approximation be disregarded when we ask for the deflection in the centre of mass system. The reason for this is, briefly, that electrons can take over little momentum but often a considerable amount of energy, because of their low mass.

We are interested in just the deflection of the ion and the recoil of the atom in the idealized elastic encounter, a so-called nuclear collision. If the ion comes close to the atom, the force is an unscreened Coulomb force and scattering is essentially given by the Rutherford formula. At larger distances of separation, however, the Coulomb force is screened, and the scattering is influenced by the field from atomic and ionic electrons.

When an ion penetrates a medium at a high velocity v, the scattering of the ion by atoms is not large and is mainly of type of Rutherford scattering. At decreasing velocity, however, the nuclear collisions at first lead to considerable multiple scattering and finally become important also in the stopping. The latter dominance occurs when the velocity v is quite low compared to the orbital velocities of electrons which could be carried by the ion, i.e. according to Thomas-Fermi estimates[17],

$$v < v_1 = Z_1^{2/3} v_0,$$

where $v_0 = e^2/\hbar$. In fact, electronic and nuclear stopping are of the same order of magnitude when[12] $v \sim 0.1 v_1$.

This implies that the problems of deviations from Rutherford scattering arise primarily when we have to do with an ion where the nuclear charge to a considerable extent is compensated by electrons carried by the ion. The nuclear charge of the atom is apparently completely screened at large distances by atomic electrons. However, the outermost electrons do not, for swift particles, compensate at the static atomic screening radius, but at slightly larger distances, because the screening contains dynamic features. We therefore envisage the interaction as a screened Coulomb field, where the screening may depend moderately on velocity. With reservations for velocity dependence, the ion-atom field is similar to the static interaction between two atoms of charge numbers Z_1 and Z_2.

Classical Scattering by Screened Potentials

Suppose that the force is known, and that the scattering is classical. The angle of scattering in the centre of mass system might then be a function of five variables, $\theta = \theta(Z_1, Z_2, v, M_0, p)$, where M_0 is the reduced mass and p the impact parameter. We are normally concerned with a conservative and central force, implying conservation of angular momentum. The classical equation of motion is then

$$\frac{d^2(R^{-1})}{d\varphi^2} + R^{-1} + \frac{R^2}{M_0 v^2 p^2} F(R) = 0, \tag{2.1}$$

where φ is the polar angle, $M_0 = M_1 M_2/(M_1 + M_2)$ the reduced mass, $F(R)$ the outward force, and $R = R(\varphi)$ the distance of separation. The initial condition, corresponding to impact parameter p, is $R^{-1} = 0$ and $d(R^{-1})/d\varphi = p^{-1}$ for $\varphi = 0$. When integrating eq. (2.1), we find that $R^{-1}(\varphi)$ increases with φ and has a maximum, whereupon it decreases and becomes zero at a certain angle, φ_1. The total deflection θ, in the centre of mass system, is then $\theta = \pi - \varphi_1$.

If the force depends on Z_1, Z_2 and distance R, the deflection θ will be a function of four variables, the velocity v and the mass M_0 having combined to one variable, $M_0 v^2$,

$$\theta = \theta(Z_1, Z_2, M_0 v^2, p). \tag{2.2}$$

The problem confronting us is whether this complicated dependence may be simplified. In the following chapters we attempt to show that, with good approximation, the number of independent variables reduces from four to one.

The first two steps in the reduction are obtained through simplifying approximations in the interaction potential.

To this end, let us consider similarity properties of interaction potentials; an approximate estimate of the potential function is given below. The ion-atom potential must be of type of

$$V(\vec{R}) = \frac{Z_1 Z_2 e^2}{R} u, \tag{2.3}$$

where the function u must tend to unity when $R \to 0$, and must vanish when $R \to \infty$, because the Coulomb potential is screened at large distances. A velocity-independent conservative potential corresponds to

$$u = u(Z_1, Z_2, R). \tag{2.4}$$

Thus, eq. (2.4) would result from a static Hartree calculation of the ground state energy of two atoms as a function of distance of separation, R. For the present purposes, however, formula (2.4) would hardly do, because the two parameters Z_1 and Z_2 correspond to an embarassingly large number of cases, of order of 10^4.

In a Thomas-Fermi treatment the static interaction between two atoms is given by

$$u = u\left(\frac{Z_1}{Z_2}, \frac{R}{a}\right), \tag{2.5}$$

where a is a characteristic screening length (cf. pp. 8–9). Formula (2.5) has one parameter less than eq. (2.4), and is therefore much simpler. When eq. (2.5) is introduced in eq. (2.1), the angle of deflection depends on three variables only,

$$\theta = \theta(Z_1/Z_2, b/a, p/a), \tag{2.6}$$

where $b = 2Z_1 Z_2 e^2/(M_0 v^2)$ is the familiar collision diameter. The parameter a/b in eq. (2.6) is used repeatedly in the following. We denote it as ε, since it is a reduced energy,

$$\varepsilon = \frac{a}{b} = \frac{a}{Z_1 Z_2 e^2} \cdot \frac{1}{2} M_0 v^2. \tag{2.7}$$

One final simplification of u may be made without introducing undue errors. Consider a simplified Thomas-Fermi potential

$$u = u\left(\frac{R}{a}\right) \quad , \tag{2.8}$$

where the dependence of u on the ratio Z_1/Z_2 in eq. (2.5) is disregarded. This simplification is actually a fairly good approximation, as discussed below (pp. 8–10).

Eq. (2.8) implies similarity of all ion-atom potentials. As a consequence, the angle of deflection obtained from eq. (2.1) becomes a function of two variables only

$$\theta = \theta\left(\varepsilon, \frac{p}{a}\right). \tag{2.9}$$

Since the differential cross section is $d\sigma = d(\pi p^2)$, it may, according to eq. (2.9), be written as

$$d\sigma = \pi a^2 \cdot F\left(\varepsilon, \sin\frac{\theta}{2}\right) d\Omega, \tag{2.10}$$

where we have introduced the variable $\sin\theta/2$ in place of θ, and where $d\Omega$ is the differential solid angle. Numerical computations of cross sections corresponding to eq. (2.10) have been made by several authors. Thus, EVERHART et al.[4] calculated scattering by the exponentially screened potential of BOHR, eq. (2.11).

The formula (2.9) shows that classical scattering by screened potentials (2.8) has comparatively simple similarity properties. Thus, suppose that in two different cases the reduced energies, ε, are the same, as well as the reduced impact parameters, p/a. We are then concerned with corresponding collisions: not only are the two deflections the same, but so are the orbits in space and time, when measured in reduced variables.

In applications of scattering formulae like (2.9), we are usually concerned with integral equations[12, 13], the integration being over the differential cross section $d\sigma$. It is then desirable to have still simpler properties, i.e. only one reduced variable instead of two in eq. (2.10). In the following, we attempt to show that this simplification may be made, retaining an accuracy which is satisfactory for most purposes. In this connection it should be remembered that already eq. (2.9) contains several consecutive approximations. If, in specified cases, one wants to improve upon standard results obtained from the simplest possible similarity description, one should not always turn to eq. (2.9), but may instead consider, e.g., the details of the Hartree treatment and of the inelastic effects.

Estimate of Ion-Atom Interaction

We shall now describe briefly the reasons for our use of an ion-atom interaction containing only one screening length, a. This type of interaction is basic to the similarity approach in the present paper, cf. the preceding section and § 4. The actual magnitude of a and its dependence on the atomic numbers Z_1 and Z_2, however, is immaterial to the similarity treatment.

In his well-known survey paper[2], NIELS BOHR discussed qualitatively many basic aspects of ion-atom collisions, and for this purpose he introduced an exponentially screened ion-atom interaction, i.e. eq. (2.3) with

$$u = \exp(-R/a_B). \tag{2.11}$$

This potential has been widely used but, when $R > a_B$, it decreases much more rapidly than do actual ion-atom interactions. For the purpose of more detailed estimates of deflections it was therefore necessary to look for a better potential. Clearly, it is possible to find a more accurate interaction, but the question is whether one can retain the simplicity of Bohr's potential, where there is only one screening parameter and similarity of all ion-atom interactions.

Before going further, we may again emphasize that the proper ion-atom interaction is a screened field containing inelastic parts and being dependent on the relative velocity. In point of fact, velocity dependence and inelastic terms are always directly connected and cannot occur independently of each other. Moreover, we have already mentioned that we are concerned mainly with cases of low velocity, where the nuclear charge of the ion is approximately neutralized by electrons. For these reasons, it would seem consistent to consider a velocity-independent, elastic interaction, and use as a guidance the static interaction between two atoms.

When asking for a potential described by one screening length, we disregard the shell structure belonging to a Hartree treatment, which again emphasizes that the static interaction obtained is to be used only as a guidance.

With these preliminaries, we can readily find the approximate shape of the potential. A static Thomas-Fermi treatment is easily seen to lead to potentials of type of (2.5), i.e. $u = u(Z_1/Z_2, R/a)$, where u is symmetric in Z_1, Z_2, and where a, at fixed ratio Z_1/Z_2, is proportional to $Z_1^{-1/3}$ (or to $Z_2^{-1/3}$)*. If one of the atomic numbers is small compared to the other, e.g.

* The proof is as follows. Suppose that the Thomas-Fermi equations are solved for atomic numbers Z_1, Z_2, and distance of separation R. We ask whether another case, $Z_1' = \alpha Z_1$, $Z_2' = \alpha Z_2$, can be solved by scaling all lengths by a factor β, e.g. $R' = \beta R$. The local potential energy of an electron is changed by α/β. The local kinetic energy is changed by $\alpha^{2/3}\beta^{-2}$, being proportional to the density to the power two thirds. Scaling is obtained when the two energies change by the same factor, i.e. for $\beta = \alpha^{-1/3}$.

$Z_1 = 1$, $Z_2 \gg 1$, the potential must be approximately the Thomas-Fermi potential of a single atom, so that in this extreme the screening function u becomes

$$u = \varphi_0(R/a), \tag{2.12}$$

where φ_0 is the Fermi function [7], and $a = 0.8853 \cdot a_0 \cdot Z_2^{-1/3}$, the number 0.8853 being a familiar Thomas-Fermi convention ($a_0 = \hbar^2/me^2$).

In order to see whether a suitable choice of a can be introduced in eq. (2.12) so as to fit approximately all cases, one need only estimate the static Thomas-Fermi interaction in the other extreme, i.e. $Z_1 = Z_2$. For this purpose, we made a detailed derivation of the potential on the basis of the perturbation method described by GOMBÁS [7]. We need not reproduce the lengthy calculations here, which also would indicate an unwarranted importance of these static calculations*. We further compared with numerical Thomas-Fermi-Dirac calculations by SHELDON [21] for $Z_1 = Z_2 = 7$, which did not deviate from the perturbation calculation by more than $\sim 10\ \%$.

When trying to see whether these numerical results for $Z_1 = Z_2$ may be approximated by eq. (2.12) with a suitable choice of $a = a(Z_1, Z_2)$, we considered Bohr's screening length as a starting-point. On the basis of qualitative considerations, BOHR suggested that the reciprocal square of the total screening length was the sum of the reciprocal squares of the screening lengths of the two atoms. It turns out that this choice reproduces fairly accurately the above-mentioned numerical results, i.e., eq. (2.12) may be applied for any pair Z_1, Z_2, with

$$a = 0.8853\, a_0 \cdot (Z_1^{2/3} + Z_2^{2/3})^{-1/2}, \tag{2.13}$$

which quantity differs from Bohr's choice only by a constant factor close to unity, $a = 0.8853\ a_B$. The formula (2.13) in (2.12) begins to deviate from the numerical estimates (cf. footnote) when R/a becomes large ($\gtrsim 5$), but this is the least important and most dubious part of the potential. The error might be remedied by not using exactly the Fermi function φ_0 at large distances.

In the following we represent the ion-atom interaction by eq. (2.12) together with eq. (2.13). We shall use various simple approximations to u, besides the Fermi function φ_0.

It is important to note that, for practical purposes, several other choices of a do not differ from eq. (2.13). Thus, suppose that we choose a screening

* The perturbation treatment, with $Z_1 = Z_2$, leads in first approximation to the interesting formula $u = \varphi_0^2(R/[2 \cdot 0.8853 \cdot a_0 \cdot Z_2^{-1/3}])$, i.e. the square of the Fermi function belonging to a single atom, but taken at half the distance of separation.

length a' proportional to $(Z_1^{1/2} + Z_2^{1/2})^{-2/3}$, instead of a in eq. (2.13). When Z_1/Z_2 changes, the ratio a'/a also changes, but this variation of a'/a is by less than $\pm 4\,\%$, and usually considerably less. We therefore found no reason to deviate from Bohr's choice of dependence on atomic numbers.

We later learned about the ingenious Thomas-Fermi estimates by Firsov [6], who derived both upper and lower limits for the potential. The reader is referred to Firsov's papers for a more detailed understanding of the static Thomas-Fermi estimates. With the qualifications mentioned above, Firsov's results are in accord with the present estimates.

In order to emphasize the uncertainties of potentials, we may quote one example. In Fig. 4 is shown the deflection by the Lenz-Jensen potential relative to that by the Thomas-Fermi potential, θ_{LJ}/θ_{TF}, as a function of impact parameter p. When p exceeds $2a$, the ratio θ_{LJ}/θ_{TF} begins to drop, and is ~ 0.75 for $p = 4a$. The Lenz-Jensen potential belongs to an isolated atom, or to $Z_1 \ll Z_2$, where it is often a better approximation to actual potentials than is the Thomas-Fermi potential, for large values of R/a [7]. This indicates the magnitude of one type of uncertainty.

Validity of Classical Estimates

The problem arises whether it is permissible to use classical mechanics in the present scattering phenomena. Usually, when posing a problem of this kind, we would have to specify completely the scattering measurement in question, in order that a well-defined answer may be given. In the present case, however, the phenomena are often classical to such a wide extent that practically all relevant calculations may be performed on the basis of classical mechanics.

To be more specific, let us consider the question whether a given total deflection, $|\theta| < 1$, may be associated with a certain impact parameter p and a classical path during the collision. For elastic collisions, this problem was discussed in a general way on the basis of wave packets in ref. 19, appendix B, in analogy to the discussion by Bohr [2]. It was shown that if we attempt to obtain a given impact parameter p and corresponding classical deflection $\theta(p)$, the minimum uncertainties in these quantities become

$$(\delta p)^2 = \frac{\lambda\!\!\!^{-}}{2|\theta'(p)|} \quad \text{and} \quad (\delta\theta)^2 = \lambda\!\!\!^{-} \cdot |\theta'(p)|. \tag{2.14}$$

If we demand that the relative uncertainty in deflection be small, $(\delta\theta)^2 < \theta^2$, we find the following condition for a classical path

$$\left| \lambda\!\!\!^{-} \cdot \frac{d}{dp} \frac{1}{\theta(p)} \right| < 1, \tag{2.15}$$

where $\lambda\!\!\!^{-} = \hbar/M_0 v$ is the wave length of the relative motion.

For a Coulomb potential, the deflection is $\theta = b/p$; when introduced in eq. (2.15), this leads to Bohr's condition

$$\varkappa = \frac{2 Z_1 Z_2 e^2}{\hbar v} > 1, \tag{2.16}$$

and if e.g. $v \ll Z_1^{2/3} e^2/\hbar$ (cf. p. 4), the condition (2.16) is amply fulfilled. For the Coulomb potential, the minimum uncertainty in impact parameter is $\delta p/p \sim (2\varkappa)^{-1/2}$, according to eq. (2.14).

In order to illustrate the general behaviour for screened Coulomb potentials, let us consider the analytically simple standard potential (4.13), where the deflection is $\theta = (b/p)\,(1 + p^2/C^2a^2)^{-1}$, $C^2 \sim 3$, i.e. according to eq. (2.15),

$$\varkappa > 1 + \frac{3p^2}{C^2a^2}, \tag{2.17}$$

which inequality indicates that at sufficiently large p, or small θ, the classical approximation becomes doubtful. In the usual case of large $\varkappa$, the inequality (2.17) is violated only at very low values of θ.

As a general result, we have found that at sufficiently high velocities, or sufficiently low angles of deflection, a quantal treatment is necessary. For several reasons, however, classical estimates may remain more reliable than indicated above. First, we often need not ask for classical trajectories, but want instead to estimate integrals of type of $\int (\sin\theta/2)^{2n} d\sigma$, $n = 1, 2$. These integrals are usually approximated well by a classical calculation when $\varkappa > 1$. Second, even at high velocities where $\varkappa < 1$, classical integrals of the above type are not completely in error, because the major part of the scattering is of Rutherford type, which formula obtains both in classical and quantal calculations. Third, we are always concerned with repulsive fields, where simple estimates are more reliable than for attractive fields.

These cursory remarks may indicate both that classical estimates are valid to a wide extent and also how, in a specified case, the error of a classical calculation can be estimated. It should be noted that we have here discussed elastic collisions only.

§ 3. Power Law Potentials and Wide Angle Extrapolation

Perturbation Calculation

We ask for a classical scattering formula with the least possible number of independent variables, with the hope to retain a reasonable accuracy. It is then tempting to consider first the familiar perturbation treatment, corresponding to forward scattering and to an approximately rectilinear path with constant velocity. Let the path be parallel to the z-axis, and let the impact parameter be p. If $K_\perp(p,z)$ denotes the force perpendicular to the path, the deflection in the centre of mass system becomes the transverse momentum transfer divided by the total momentum, i.e*.

$$\theta = \frac{1}{M_0 v^2}\int_{-\infty}^{\infty} K_\perp(p,z)dz = -\frac{1}{M_0 v^2}\frac{\partial}{\partial p}\int_{-\infty}^{\infty} V([p^2+z^2]^{1/2})dz, \tag{3.1}$$

if $\theta \ll 1$. The angle θ is therefore obtained from the potential V by one integration and one differentiation. Consider a screened Coulomb potential (2.3) of type of eq. (2.8), where the potential is a function containing only one parameter, R/a. We then find from formula (3.1)

$$\theta = \frac{b}{p} g\left(\frac{p}{a}\right) \quad , \tag{3.2}$$

where $b = 2Z_1 Z_2 e^2/M_0 v^2$ is the collision diameter, and

$$g(\zeta) = \int_0^{\pi/2} \cos\varphi d\varphi \left\{ u\left(\frac{\zeta}{\cos\varphi}\right) - \frac{\zeta}{\cos\varphi} u'\left(\frac{\zeta}{\cos\varphi}\right)\right\}. \tag{3.3}$$

The formulae (3.1) and (3.2) may also be obtained from eq. (2.1), if the last term on the left in eq. (2.1) is considered as a perturbation. Note that in the case of an unscreened Coulomb potential, one has $u(R/a) = 1$ and therefore $g = 1$.

As to the number of variables necessary in a perturbation treatment, we find from eq. (3.2), since $a/b = \varepsilon$,

$$\varepsilon \cdot \theta = \frac{a}{p} \cdot g\left(\frac{p}{a}\right) \quad . \tag{3.4}$$

* The reader may notice that the integrated potential on the right-hand side of eq. (3.1) is of importance also in small angle quantal scattering[18], and in directional effects for crystal lattices[19], where it is proportional to the continuum potential, $U(r) = d^{-1}\int_{-\infty}^{\infty} V((r^2+z^2)^{1/2})dz$, the constant d being the distance between atoms along the particle path.

The number of independent variables is therefore reduced by one in the perturbation treatment, i.e. from two in eq. (2.9) to one—p/a—in eq. (3.4), because the dependent scattering variable has become $\varepsilon\theta$. This similarity in dependence of scattering on energy for $\theta \ll 1$ we now wish to extend to scattering by finite angles θ.

If the scattering potential depends also on Z_1/Z_2, i.e. if eq. (2.5) holds, we find that $g = g(Z_1/Z_2, p/a)$, so that $\varepsilon \cdot \theta$ in eq. (3.4) depends on two variables, which again is one variable less than in the exact solution (2.6) belonging to the potential (2.5).

Power Law Potentials

In order to see whether scattering by finite angles may also permit a reduction in the number of variables, we study at first in some detail the case of power law potentials, $V(R) \propto R^{-s}$, or

$$u\left(\frac{R}{a}\right) = \frac{k_s}{s} \cdot \left(\frac{a}{R}\right)^{s-1}, \tag{3.5}$$

where k_s is a constant. One of the advantages of power law potentials is that, for several integer values of s, there are simple exact scattering formulae, so that it becomes easy to estimate the accuracy of approximate solutions.

In limited intervals of R, screened Coulomb potentials like eq. (2.3) may be represented by power law potentials, i.e. $s = -\partial \log V/\partial \log R$. For low values of R, the power s must approach the value 1 belonging to an unscreened Coulomb potential. In a considerable region of R-values, s is of order of 2 or 3.

From eqs. (3.5), (3.2) and (3.3) we find for the deflection

$$\theta = \gamma_s \cdot b \cdot a^{s-1} k_s \frac{1}{p^s} \quad , \quad \text{if} \quad \theta \ll 1, \tag{3.6}$$

where

$$\gamma_s = \int_0^{\pi/2} \cos^s \varphi d\varphi = \frac{\Gamma\left(\frac{1}{2}\right)\Gamma\left(\frac{s+1}{2}\right)}{2\Gamma\left(\frac{s}{2}+1\right)} = \frac{1}{2} B\left(\frac{1}{2}, \frac{s+1}{2}\right), \tag{3.7}$$

$B(x,y)$ being the beta function[3]. From the explicit formula for γ_s in terms of gamma functions, one derives the useful relation $\gamma_s \cdot \gamma_{s-1} = \pi/(2s)$. It

follows then that $s \cdot \gamma_s = (s-1) \cdot \gamma_{s-2}$. Table 1 gives values of γ_s in a number of representative cases; we are only interested in cases where $s \geq 1$. In § 5 we attempt to approximate γ_s by simple functions.

TABLE 1. Values of $\gamma_s = \frac{1}{2} B\left(\frac{1}{2}, \frac{s+1}{2}\right)$.

s	1	1.5	2	2.5	3	4	5	∞
γ_s	1	0.874	$\pi/4$	0.719	2/3	$3\pi/16$	8/15	$\sqrt{\pi/2s}$

Wide Angle Extrapolation

At small angles of deflection, it is not important to select carefully the variables which are to characterize the scattering. In the above, we chose as variables the angle θ and the impact parameter p. In the case of finite angles of deflection, we may note, first, that the differential cross section $d\sigma = d(\pi p^2)$ is preferable to the variable p. Second, we usually want to integrate functions of T times the probability of scattering, where T is the energy transfer in the laboratory system[2], $T = T_m \cdot \sin^2 \theta/2$, T_m being the maximum energy transfer in elastic collisions. In terms of T, the differential cross section (2.10) becomes, according to eq. (3.6),

$$d\sigma = -\pi \left\{ \frac{b^2}{4} a^{2s-2} k_s^2 \gamma_s^2 T_m \right\}^{1/s} \cdot \frac{1}{s} \frac{dT}{T^{1+1/s}}, \tag{3.8}$$

and we expect this formula to be more appropriate than eq. (3.6), at wide angles of deflection. It so happens that for Coulomb potentials the formula (3.8) is exactly the Rutherford law (cf. below), and it is therefore worth while to consider the consequences of (3.8) in some detail.

Even though eq. (3.8) is derived from the perturbation formula (3.6), there is considerable difference between the two, at finite angles θ. Firstly, in eq. (3.8) θ is replaced by $2 \sin \theta/2$, as described above. Secondly, eq. (3.8) is obtained from formula (3.6) by differentiation of p^2, so that p^2 in eq. (3.6) might contain an arbitrary additive constant, $p^2 \to p^2 + p_0^2$, and still lead to eq. (3.8). Therefore, eq. (3.8) is equivalent to

$$2 \sin \frac{\theta}{2} = \gamma_s \cdot b \cdot a^{s-1} k_s \cdot (p^2 + p_0^2)^{-s/2}, \tag{3.9}$$

where p_0^2, so far, is an arbitrary constant. The obvious demand that $T \leq T_m$ in eq. (3.8), or that $\sin \theta/2 \leq 1$ in eq. (3.9), leads to fixation of p_0. For

repulsive potentials we have $\sin\theta/2 = 1$ for $p = 0$, so that, according to eq. (3.9), $p_0^2 = (\gamma_s \cdot b \cdot a^{s-1} k_s/2)^{2/s}$ *. The introduction of p_0 implies, qualitatively, that for a given impact parameter p we have introduced an effective closest distance of approach, $\sim (p^2 + p_0^2)^{1/2}$. We describe eq. (3.9), or eq. (3.8) with $0 \leq T \leq T_m$, as the wide angle extrapolation.

Accuracy of Wide Angle Extrapolation

It remains to study the accuracy of eq. (3.9). Let us consider $s = 1$, i.e. an unscreened Coulomb potential. In this case, $u = 1$ in eq. (3.5) and therefore $k_1 = 1$. Since also $\gamma_1 = 1$, we find that $p_0 = b/2$. Thus, eqs. (3.8) and (3.9) are seen to contain the exact Rutherford formula.

Let us next compare eq. (3.8) with exact scattering in another potential of considerable interest, i.e. a repulsive R^{-2}-potential. A straightforward comparison shows that in this case the differential cross section (3.8) agrees well with the exact classical scattering (cf. Bohr, ref. 2, eq. (1.5.5)), the error increasing from 0 at $T = 0$, to $-3\,\%$ at $T = T_m$, corresponding to backward scattering.

More generally, it turns out that—independently of the value of s—the relative error in eq. (3.8) is largest at $T = T_m$, and decreases towards zero when T tends to zero. Let us therefore consider the error belonging to backward scattering as a function of s. When s increases from 1, the relative error in eq. (3.8) for backward scattering rises slowly from 0 to $\sim 15\,\%$ at $s = 3/2$, whereupon it decreases to 0 at $s \approx 2$, and becomes $-20\,\%$ at $s = 5/2$. For higher s-values it becomes increasingly negative. As a result, we find that in the region $1 < s < 5/2$ the formula (3.8) is sufficiently accurate for our purposes, even for large energy transfers T. For values of s higher than $\sim 5/2$, the accuracy is not good in the limit of extreme backward scattering.

The power law potentials give only a first guidance, since we wish to study screened Coulomb potentials, where the effective power s increases slowly from 1 at small values of R/a, to $s \sim 2$ when $R/a \sim 1$ and, finally, to $s \sim 3$–4 at large distances where $R/a \gg 1$. At low energies, the collisions become less penetrating, and the scattering by screened Coulomb potentials is determined by regions with high values of s. Since the present method underestimates the backward scattering in such regions, it might seem as

* We have thus found that θ is a function of only one variable $\xi_s = b \cdot a^{s-1} k_s / p^s$. This is also correct in an exact description of scattering by R^{-s}-potentials. The exact formulae for the dependence of θ on ξ_s deviate from the comprehensive formula (3.9), but deviations are quite small at low s-values, as shown in the text.

if scattering integrals are seriously underestimated at low energies. For several reasons, however, we expect that such errors are much reduced. First, at any given energy the backward scattering concerns the closest collisions, i.e. the lowest effective power s. Second, a reduced accuracy merely in the region $\theta \approx \pi$ does not impair most estimates of scattering integrals. In this connection, it is also important that backward scattering events can remain rare even during the whole process of slowing-down, and thus need not contribute much to the dominating part of the probability distribution of, e.g., energy loss. Third, it should be remembered that inelastic effects can be important just in the case of backward scattering, so that here we may not need the highest possible accuracy in the approximation of elastic collisions. It seems therefore worth while to accept the procedure of extrapolation to wide angles used in eqs. (3.8) and (3.9), and apply it to actual potentials with the hope that, by and large, errors are less than, say, $10\,\%$.

§ 4. Scattering Formula for Screened Coulomb Potentials

Before treating actual examples of screened potentials, we introduce a terminology suitable for the similarity treatment belonging to the wide angle extrapolation. If we apply the wide angle extrapolation to eq. (3.4), its left-hand side becomes $\varepsilon \cdot 2 \sin \theta/2$, so that in the differential cross section, (2.10), the function $\varepsilon^{-2} F$ depends only on this variable. We therefore introduce a parameter t given by

$$t = \varepsilon^2 \cdot \sin^2 \theta/2, \quad \varepsilon = a/b. \tag{4.1}$$

The parameter t is proportional to the energy transfer T times the particle energy E, $t = T \cdot E \cdot (M_2/M_1) \cdot (2 Z_1 Z_2 e^2/a)^{-2}$.

We may now rewrite the differential cross section (2.10) in the following form

$$d\sigma = -\pi a^2 \frac{dt}{2 t^{3/2}} f(t^{1/2}), \tag{4.2}$$

whereby we have defined a scaling function $f(t^{1/2})$. We have introduced the factor $t^{3/2}$ in the denominator for practical purposes: the case of power law scattering with $s = 2$ then corresponds to $f = \text{const}$. In the inner parts of the atom where $s < 2$, the function f therefore decreases for increasing t; in the outer parts of the atom, where $s > 2$, f increases with increasing t. Now, t in itself is a measure of the depth of penetration into the atom, large values of t corresponding to small distances of approach. We therefore

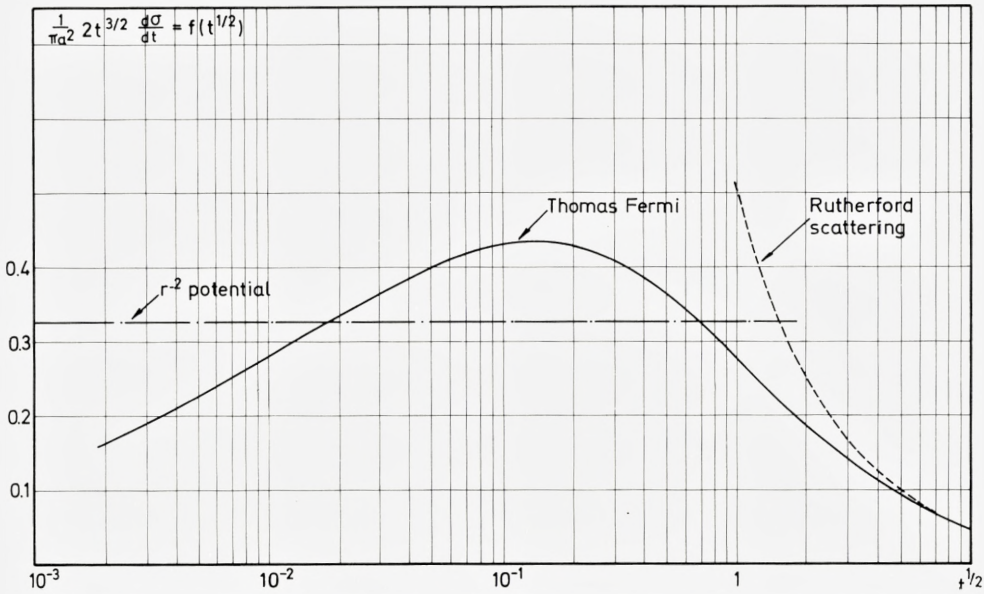

Fig. 1. Reduced differential cross section, calculated from Thomas-Fermi potential and eqs. (4.3) and (4.4). Ordinate is $f(t^{1/2}) = 2t^{3/2}(d\sigma/dt)\cdot(\pi a^2)^{-1}$; abscissa is $t^{1/2} = \varepsilon \sin\theta/2$. For large values of $t^{1/2}$, curve approaches Rutherford scattering, indicated by dashed curve. Horizontal line represents f for R^{-2}-potential.

expect that f increases for small values of t until it reaches a maximum, and decreases for large values of t.

In order to treat scattering by a screened Coulomb potential, we must specify the wide angle extrapolation of the general perturbation formula (3.4). By means of the procedure leading to eq. (3.9), we find directly

$$t^{1/2} = \varepsilon \cdot \sin\theta/2 = \frac{1}{2} \frac{a}{(p^2 + p_0^2)^{1/2}} g\left(\frac{1}{a}(p^2 + p_0^2)^{1/2}\right), \tag{4.3}$$

where $p_0 = p_0(\varepsilon, a)$ has become a redundant parameter, which need not be determined. If we know the screening function u, we can compute g from eq. (3.3) by one differentiation and one integration. Next, we solve eq. (4.3) with respect to $p^2 + p_0^2$, i.e. $p^2 + p_0^2(\varepsilon, a) = a^2 \cdot G(t^{1/2})$. Having obtained $G(t^{1/2})$, we derive $f(t^{1/2})$ in (4.2) by differentiation

$$f(t^{1/2}) = -t \cdot G'(t^{1/2}). \tag{4.4}$$

This calculation of the universal scattering function f is normally done numerically.

TABLE 2a.
Thomas-Fermi scattering function $f(t^{1/2})$, cf. text and Fig. 1.

$t^{1/2}$	$f(t^{1/2})$
0.002	0.162
0.004	0.209
0.01	0.280
0.02	0.334
0.04	0.383
0.10	0.431
0.15	0.435
0.20	0.428
0.40	0.385
1	0.275
2	0.184
4	0.107
10	0.050
20	0.025
40	0.0125

TABLE 2b.
Thomas-Fermi $s(\varepsilon)$ and $w(\varepsilon)$, cf. text and Figs. 2 and 3.

ε	$s(\varepsilon)$	$w(\varepsilon)$
0.002	0.120	0.000097
0.004	0.154	0.00025
0.01	0.211	0.00085
0.02	0.261	0.00206
0.04	0.311	0.00479
0.10	0.372	0.0138
0.15	0.393	0.0214
0.20	0.403	0.0287
0.40	0.405	0.0542
1	0.356	0.105
2	0.291	0.152
4	0.214	0.189
10	0.128	0.228
20	0.0813	0.245
40	0.0493	0.249

In our basic numerical computation of f, we have chosen the Thomas-Fermi potential ($u(\xi) = \varphi_0(\xi)$). It turns out that for very low values of t the function $f(t^{1/2})$ behaves asymptotically as $\sim 1.43 \cdot (t^{1/2})^{0.35}$. The results are shown in Table 2a and Fig. 1, the latter representing $f(t^{1/2})$ as a function of $t^{1/2}$. In the figure is also shown the asymptotic Rutherford scattering, $f = 1/(2t^{1/2})$, as well as a horizontal line corresponding to power law scattering with $s = 2$, and $k_2 = 2/(0.8853e)$, i.e. the value of k_2 chosen by BOHR [2].

It is apparent that the treatment is inaccurate at low values of ε, e.g. $\varepsilon < 10^{-2}$. In particular, at such low values of ε the case of low atomic numbers Z_1 and Z_2 corresponds to particularly low energies, where deviations from Thomas-Fermi estimates may be considerable.

Stopping Cross Sections and Fluctuations[12]

Having obtained the scattering cross section in terms of $f(t^{1/2})$, we may next calculate the stopping cross section S for nuclear collisions given by

$$S = \int T d\sigma = T_m \cdot \int \sin^2 \frac{\theta}{2} d\sigma, \tag{4.5}$$

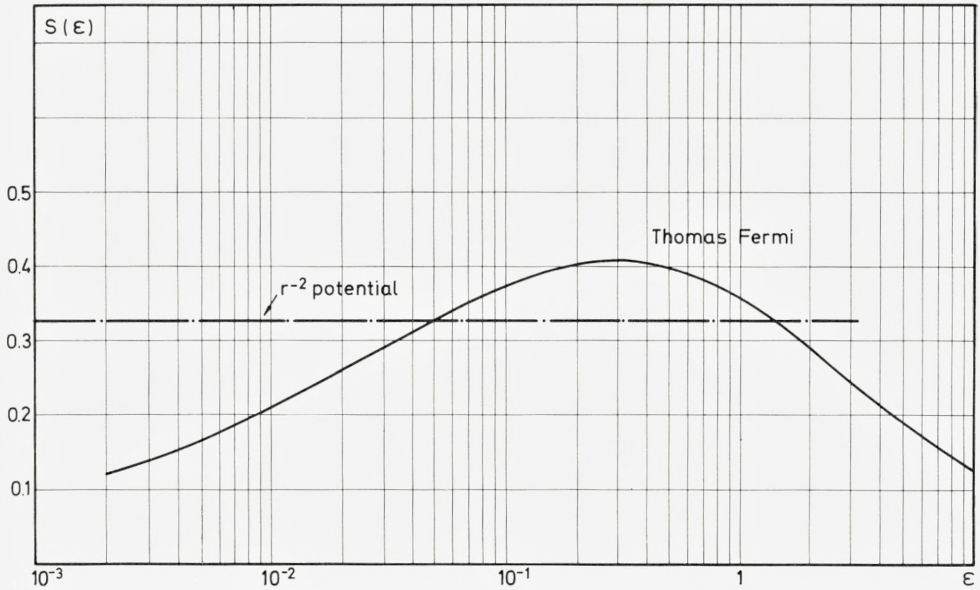

Fig. 2. Reduced nuclear stopping cross section s, (4.7), as function of ε. Curve obtained by integration (4.8) of Thomas-Fermi curve in Fig. 1. Horizontal line represents s for R^{-2}-potential.

where T is the energy transfer to an atom at rest, and $T_m = E \cdot 4M_1M_2 \cdot (M_1+M_2)^{-2}$ is the maximum value of T. The stopping cross section S may be associated with the specific energy loss, $S(E) = (dE/dR) \cdot N^{-1}$, where N is the number of atoms per unit volume and dR the differential path length, R being the range measured along the path. It is seen that if we define a reduced range, ϱ, by

$$\varrho = RNM_2 \cdot 4\pi a^2 \frac{M_1}{(M_1+M_2)^2}, \tag{4.6}$$

we may introduce a reduced stopping cross section $s(\varepsilon)$ by means of the equation

$$s(\varepsilon) = \frac{dE}{dR} \cdot \frac{\varepsilon}{E} \cdot \frac{R}{\varrho} \quad . \tag{4.7}$$

We consider only nuclear stopping in (4.7), and find from (4.2) and (4.5)

$$s(\varepsilon) = \frac{1}{\varepsilon} \int_0^{\varepsilon} f(\zeta) d\zeta. \tag{4.8}$$

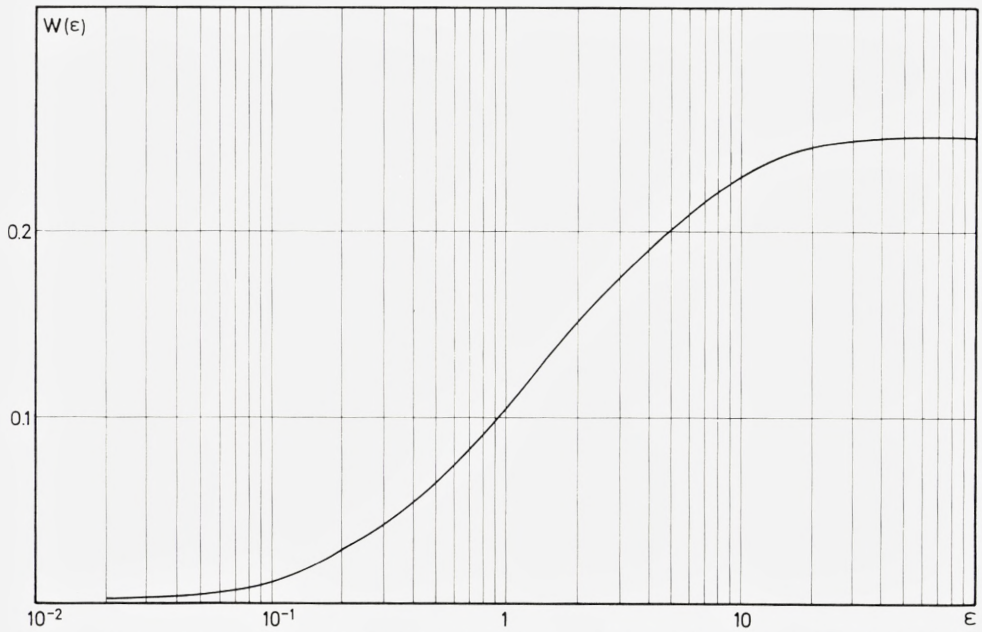

Fig. 3. Reduced square fluctuation in energy loss $w(\varepsilon)$, obtained from eq. (4.9) and Thomas-Fermi $f(t^{1/2})$.

In Fig. 2 and Table 2b is shown the reduced stopping cross section (4.8) as a function of ε, computed from the Thomas-Fermi estimate of f given in Fig. 1 and Table 2a; for $\varepsilon \gtrsim 10$ one finds approximately $s = (2\varepsilon)^{-1} \log(1.294\varepsilon)$. The corresponding square fluctuation in reduced energy loss,

$$w(\varepsilon) = \frac{1}{\varepsilon^2} \int_0^{\varepsilon} \zeta^2 f(\zeta) d\zeta, \tag{4.9}$$

is shown in Fig. 3 and Table 2b.

It may be noted that a stopping cross section depending on the variable ε obtains not only from the one-parameter cross section (4.2), but also from the two-parameter cross section (2.10). If so desired, we would in fact—by differentiation of $\varepsilon \cdot s(\varepsilon)$ in eq. (4.8)—be able to find a function $f(t^{1/2})$ in eq. (4.2) which gives exactly the same stopping cross section as a two-parameter scattering formula, (2.10).

It should be appreciated that in many cases one is not concerned with the total nuclear stopping cross section (4.8). Since the probability of the closest collisions is low, these collisions may correspond to a tail in the energy loss

distribution. If one then observes the most probable energy loss, this quantity may be obtained from the integration in eq. (4.8) with an upper limit smaller than ε. The simplicity of the present description in such cases was utilized by FASTRUP et al.[5].

Power Law Scattering

In the case of power law potentials, eq. (3.5), the formula (3.8) leads to

$$f(t^{1/2}) = \lambda_s \cdot t^{\frac{1}{2}-\frac{1}{s}}, \tag{4.10}$$

where the constant $\lambda_s = (2/s)(k_s\gamma_s/2)^{2/s}$ depends on γ_s given by eq. (3.7). In particular, $\lambda_1 = k_1^2/2$, so that $f = t^{-1/2}/2$ for Rutherford scattering, and for $s = 2$ we find $f = \lambda_2$, where $\lambda_2 = k_2\pi/8$. It turns out that $0.3 \lesssim \lambda_s \lesssim 1.5$, and $1 \leq s \lesssim 3$, in the important regions of screened Coulomb interactions*.

Whereas the power law scattering (3.8) was derived as an approximate description of scattering by power law potentials, we may turn the tables and consider the power law scattering as a basic approximation without bothering about the question of an associated potential. Power law scattering has proved useful in analytic treatments of integral equations[12, 13, 22]. The only restriction we put on the power law scattering is that $s \geq 1$, so that it is never more strongly peaked in the forward direction than corresponding to Rutherford scattering. Thus, according to eq. (4.10) or (3.8), the differential cross section $d\sigma/dT$ is proportional to T to a power between T^{-1} and T^{-2}. The present scattering by screened Coulomb fields must therefore always remain quite different from isotropic scattering, where $d\sigma/dT$ is constant.

For power law scattering the reduced stopping cross section (4.8) becomes

$$s_s(\varepsilon) = \frac{\lambda_s}{2\left(1-\frac{1}{s}\right)} \cdot \varepsilon^{1-\frac{2}{s}}. \tag{4.11}$$

Again, the case of power law scattering for $s = 2$ is particularly simple, since $s_2(\varepsilon) = \lambda_2 = \text{const}$.

Comparison of Deflections by Various Potentials

A comparison between deflections by various screened potentials is shown in Fig. 4. The deflections are measured relative to the corresponding

* For small t, the asymptotic behaviour of the Thomas-Fermi scattering function in Table 2a corresponds to $s \approx 3.1$ and $\lambda \approx 1.43$, whereas the standard potential, (4.13), leads to $s \to 3$, $\lambda \to 0.87$.

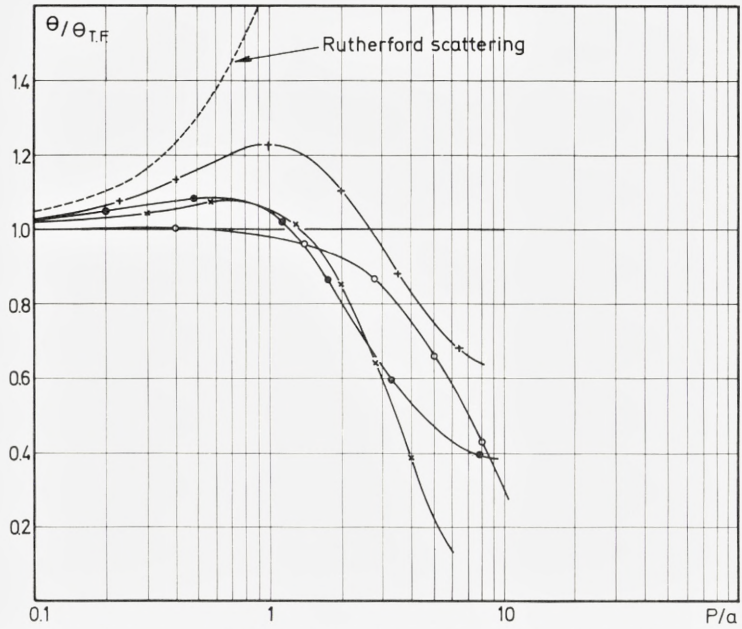

Fig. 4. Comparison between deflections by various screened potentials. At a given energy ε, ordinate θ/θ_{TF} represents deflection measured relative to deflection for Thomas-Fermi potential. Abscissa is reduced impact parameter p/a. The curves shown are Lenz-Jensen potential: ○, Bohr potential: ×, standard potential, $C^2 = 3$: +, and $C^2 = 1.8$: ●.

deflection in a Thomas-Fermi potential at the same energy E, so that the ordinate is the ratio θ/θ_{TF}. The abscissa is the reduced impact parameter, p/a. The comparison in Fig. 4 therefore belongs to the perturbation case, where deflections are small. The curves were calculated from the magic formula, cf. § 5. It may be added that the curves in Fig. 4 are actually applicable at all angles of deflection, if the ordinate is interpreted as $(t/t_{TF})^{1/2}$ and the abscissa as $(p^2+p_0^2)^{1/2}/a$.

The curve with open circles represents the Lenz-Jensen potential. It follows the Thomas-Fermi potential rather well until $p/a \sim 2$, and then drops considerably below it. Although the Lenz-Jensen potential belongs to single atoms, the curve indicates that the Thomas-Fermi potential may overestimate scattering at large impact parameters. The curve for the Bohr potential (×) is slightly too high when $p/a < 1$, but is much too low when $p/a > 2$.

The figure also indicates the relative deflection by the 'standard potential'. For several purposes it has been useful to approximate the screened ion-

atom interaction by a simple function, which we have called standard potential[18, 19],

$$u(R/a) = 1 - \frac{R}{(R^2 + C^2 a^2)^{1/2}} \quad . \tag{4.13}$$

The standard potential contains one adjustable parameter, C. A fairly good over-all fit is obtained for the usual choice, $C^2 = 3$. The standard potential is much simpler analytically than the Bohr potential and also a better approximation to the Thomas-Fermi potential.

In Fig. 4, the curve for the standard potential with $C^2 = 3$ (+) is too high when $p/a \sim 1$, but at high values of p/a it has the merit of being between Thomas-Fermi and Lenz-Jensen. For comparison is also shown a curve for the standard potential with $C^2 = 1.8$ (full circles). It follows the Bohr potential rather closely when $p/a < 2$, but for higher values of p/a it is less in error than is the Bohr potential.

Wide Angle Extrapolation for Attractive Potentials

In the perturbation case, eq. (3.1), the magnitude $|\theta|$ of the deflection is independent of the sign of the potential. This holds no longer at finite angles—except for unscreened Coulomb potentials—and the wide angle approximation (3.9) and (4.3) is applicable only for repulsive potentials. It may be worth while to indicate that a similar wide angle approximation may be introduced for attractive potentials, but it does not possess the accuracy belonging to repulsive potentials. Consider the extrapolation of eq. (3.6) for attractive potentials, and demand again that Rutherford scattering is obtained exactly. We are then led to the substitution $\theta \to 2tg\theta/2$, i.e. instead of eq. (3.9) we get $2tg\theta/2 = \gamma_s \cdot b \cdot a^{s-1} k_s \cdot p^{-s}$. For general screened potentials we therefore introduce, instead of t in eq. (4.1), the parameter $t^* = \varepsilon^2 \cdot tg^2\theta/2$, with $\varepsilon = a/b$. The differential cross section is determined by eq. (4.2), where t is replaced by t^*, the function f being given e.g. in Fig. 1. This simple approximation may sometimes be useful (for large ε), but as a general rule it is not particularly accurate.

Approximations by Other Authors

During later years, several authors have discussed approximation methods in elastic scattering by screened repulsive Coulomb fields (cf. e.g. refs. 1, 6, 8, 9, 10, 23). Heinrich[8] has suggested an interesting interpolation between forward and backward scattering which has some resemblance to our treatment. His results may be more accurate than ours, but do not contain the similarity property which is the main simplification in the present work. Both Leibfried et al.[9] and Smith et al.[23] have studied a series expansion valid at small angles only and an expansion valid only for θ in the neighbourhood of π. Biersack[1] has made scattering calculations where he comments on some of the present results.

§ 5. Magic Formula for Scattering

The above method of calculating $f(t^{1/2})$ for screened potentials by means of the perturbation formula (3.1) was used in our original computations of stopping powers and cross sections. We have therefore reproduced that calculation in § 4. Shortly after having applied the formulae, we did, however, derive a much simpler method. We called it the magic formula, because its structure and accuracy was rather surprising. In the present chapter we introduce the magic formula and use it for a number of comparative studies. We shall find that it gives quite closely the same results as found in § 3 and § 4.

Power Potentials

As a starting-point, we consider again the perturbation formula for scattering by power law potentials, i.e. eq. (3.6). We note that, since the deflection is $\theta = \gamma_s b k_s p^{-s} a^{s-1}$, it is proportional to the potential $V_s(R)$ itself (cf. eqs. (2.3) and (3.5)), taken at the distance $R = p$, and multiplied by $s \cdot \gamma_s$. Now, a multiplication by s is equivalent to a logarithmic differentiation, $-Rd/dR$, of the power law potential. Therefore, if γ_s may be approximated by a simple function of s, we should be able to obtain the right-hand side of eq. (3.6) by differentiation of the potential at the point $R = p$, or by integration. When looking for a simple approximation to γ_s, we can hardly avoid introducing a square root, because of the asymptotic behaviour given in Table 1, i.e. $\gamma_s \to (\pi/2s)^{1/2}$ for $s \to \infty$. We must also demand that the approximation is accurate for $s = 1$, where $\gamma_s = 1$. Let us compare two fairly accurate approximations of this type, denoted as γ_s' and γ_s'',

$$\gamma_s' = \frac{1}{s}\sqrt{\frac{3s-1}{2}}, \tag{5.1}$$

and

$$\gamma_s'' = \sqrt{\frac{\pi}{2s+1}}. \tag{5.2}$$

Both of the functions represent rather well the asymptotic behaviour of γ_s for $s \to \infty$. When $s = 1$, we find $\gamma_1' = 1$, which is the correct value, whereas $\gamma_1'' = 1.023$, i.e. slightly too large. It is of course an advantage that Rutherford scattering ($s = 1$) is obtained exactly. The behaviour of the ratios γ_s'/γ_s and

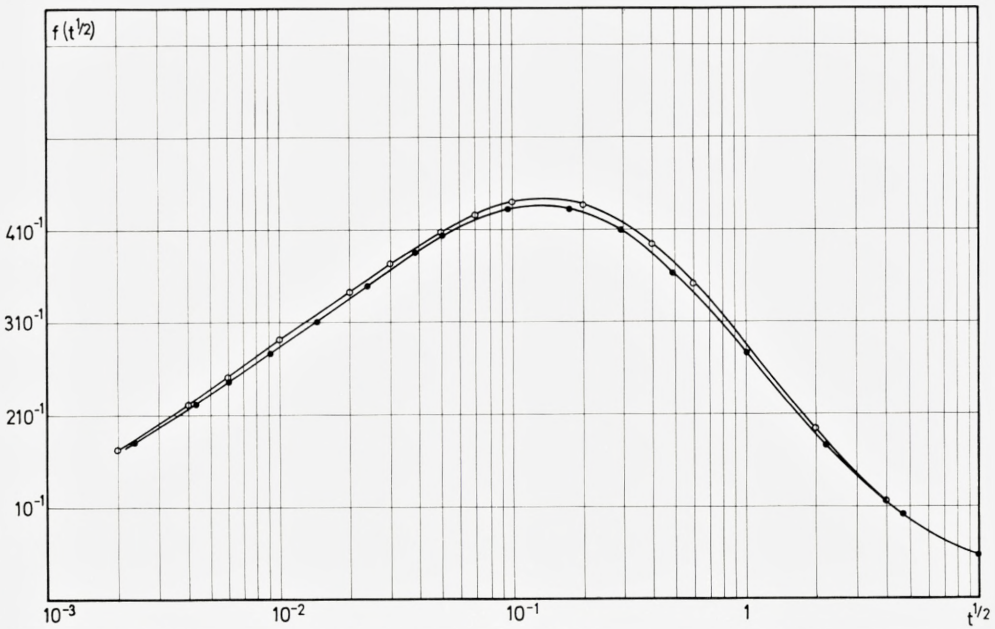

Fig. 5. Check of error in magic formula applied to Thomas-Fermi potential. Curve with open circles reproduces $f(t^{1/2})$ as a function of $t^{1/2}$ from Fig. 1. Curve with full circles is calculated from magic formula, eqs. (5.4) and (5.5).

γ_s''/γ_s is stated in Table 3. It is apparent that γ_s' gives a superior fit—within $1\,{}^0/_0$—in the important interval $1 \leq s \leq 4$, and γ_s' coincides with γ_s not merely for $s = 1$, but also for $s = 3$.

TABLE 3.
Accuracy of γ_s', (5.1), and γ_s'', (5.2).

s	1	1.5	2	2.5	3	4	5	6	∞
γ_s'/γ_s	1.000	1.009	1.007	1.002	1.000	0.995	0.992	0.990	0.977
γ_s''/γ_s	1.023	1.016	1.009	1.007	1.004	1.003	1.002	1.002	1

The decisive feature, however, is the way in which s enters in the two functions. The significant quantity is $s \cdot \gamma_s$, as shown above, and γ_s' has the property that $(s\gamma_s')^2 = (3s-1)/2$, which corresponds simply to one differentiation. The quantity $(s\gamma_s'')^2 = \pi s^2/(2s+1)$, on the contrary, is of a type requiring one integration and two differentiations, and is therefore quite

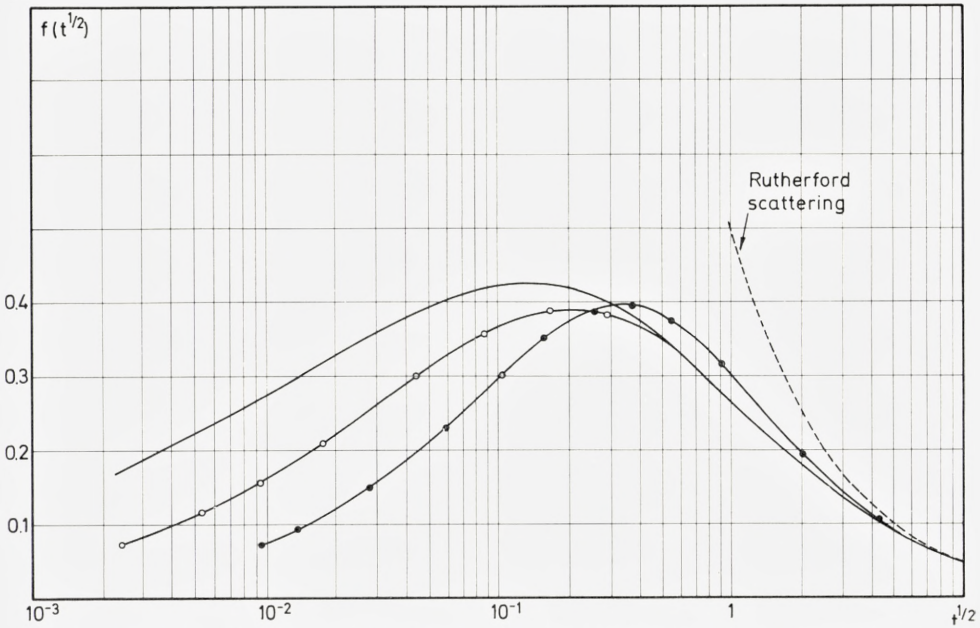

Fig. 6. Comparison of reduced differential cross sections for three screened Coulomb potentials. Ordinate is $f(t^{1/2}) = 2t^{3/2}(d\sigma/dt)(\pi a^2)^{-1}$, abscissa is reduced deflection $t^{1/2} = \varepsilon \sin\theta/2$. Full-drawn curve corresponds to Thomas Fermi potential, curve with open circles to Lenz-Jensen potential, and curve with full circles to Bohr potential, (2.11).

complicated. Although we might have made the numerical values of γ_s'' as accurate as those of γ_s' by introducing a constant factor, this would not improve upon the innate complication belonging to γ_s''.

Magic Formula in Perturbation Limit

On the basis of γ_s' in eq. (5.1), we are then led to a tentative perturbation formula for scattering, as deduced from power law potentials,

$$\frac{\theta^2}{4} = -\frac{3}{4(M_0 v^2)^2} p^{1/3} \frac{d}{dp}\{V^2(p)p^{2/3}\}. \tag{5.3}$$

We have seen that, in so far as γ_s' may be considered equal to γ_s, the formula (5.3) is equivalent to the perturbation formula (3.6) for power potentials. In particular, for $s = 1$ and $s = 3$ the two formulae coincide; the error in θ is less than $1\,\%$ when $s \leq 6$, and less than $\sim 2\,\%$ when s is large.

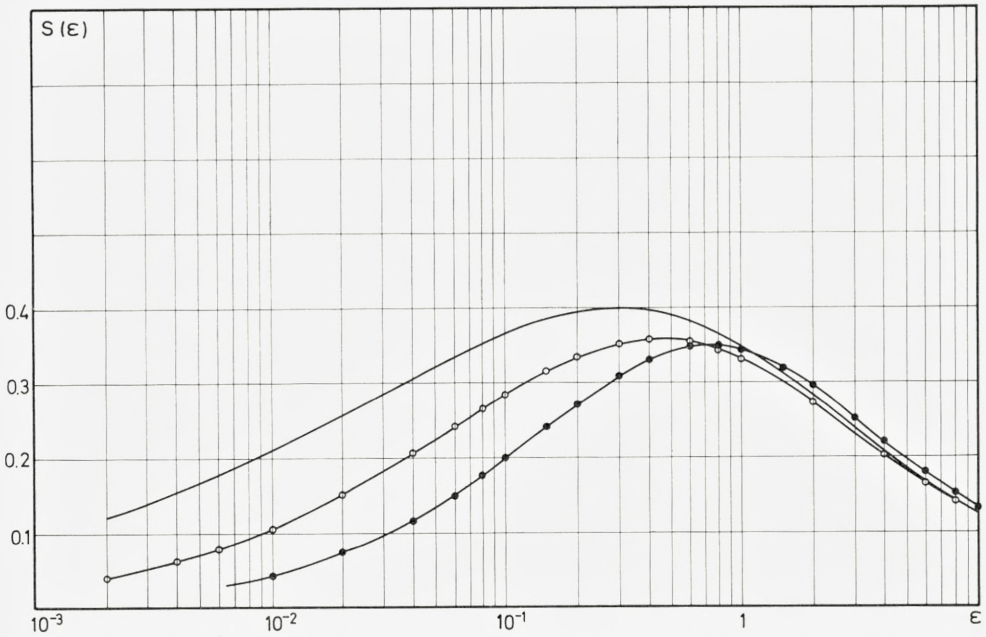

Fig. 7. Comparison of reduced stopping cross section, $s(\varepsilon)$, for three screened Coulomb potentials, calculated from curves in Fig. 6. Full-drawn curve corresponds to Thomas-Fermi potential, open circles to Lenz-Jensen potential, and full circles to Bohr potential.

We shall show presently that—in the general case of screened Coulomb potentials—the formula (5.3) rather faithfully reproduces the original perturbation formula (3.1). The advantage of eq. (5.3) is that only one differentiation is necessary, whereas eq. (3.1) demands one differentiation and one integration. The magic formula (5.3) is therefore primarily an alternative way of calculating scattering by small angles, the advantage being great simplicity in both analytical and numerical treatments.

Magic Formula Applied to Wide Angles

We can immediately generalize the perturbation formula (5.3) by introducing the wide angle extrapolation (3.9). We replace $\theta^2/4$ in eq. (5.3) by $\sin^2\theta/2$, and the impact parameter p by $(p^2+p_0^2)^{1/2}$, where $p_0 = p_0(E)$. We confine the treatment to the basic case of a screened Coulomb potential given by eq. (2.8), i.e. $V(R) = Z_1Z_2e^2u(R/a)/R$. By changing to reduced variables, we then arrive at a formulation of eq. (5.3) which includes wide angles,

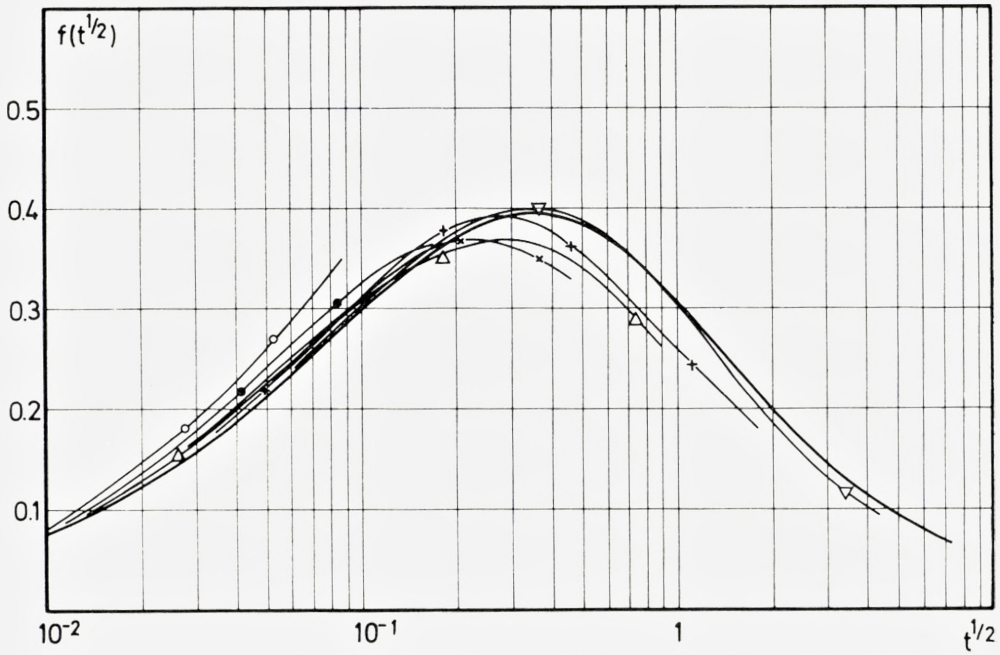

Fig. 8. Comparison between exact calculations (EVERHART et al.[4]) and present formulae for Bohr potential, in a $f(t^{1/2})$ vs. $t^{1/2}$-plot. Full-drawn curve is calculated from magic formula. The six separate curves are Everhart's calculations, for $\varepsilon = 0.089$ (○), $\varepsilon = 0.177$ (●), $\varepsilon = 0.443$ (×), $\varepsilon = 0.89$ (△), $\varepsilon = 1.77$ (+), and $\varepsilon = 4.43$ (▽).

$$t = \varepsilon^2 \sin^2 \frac{\theta}{2} = -\frac{3}{16} \xi^{1/3} \frac{d}{d\xi} \{u^2(\xi) \xi^{-4/3}\}, \tag{5.4}$$

which connects t with the variable $\xi = (p^2/a^2 + p_0^2/a^2)^{1/2}$, by means of a differentiation. According to the definition of $f(t^{1/2})$, eq. (4.2), we find this function from eq. (5.4) by one further differentiation,

$$f(t^{1/2}) = -\frac{2t^{3/2}}{dt/d(\xi^2)}. \tag{5.5}$$

The formulae (5.4) and (5.5) represent the magic formula in the case of wide angle extrapolation for repulsive potentials.

Fig. 5 gives a comparison between the direct calculation of $f(t^{1/2})$ for the Thomas-Fermi potential, as given in Fig. 1, and a calculation by means of the magic formula. The deviations in the cross section are seen to be less

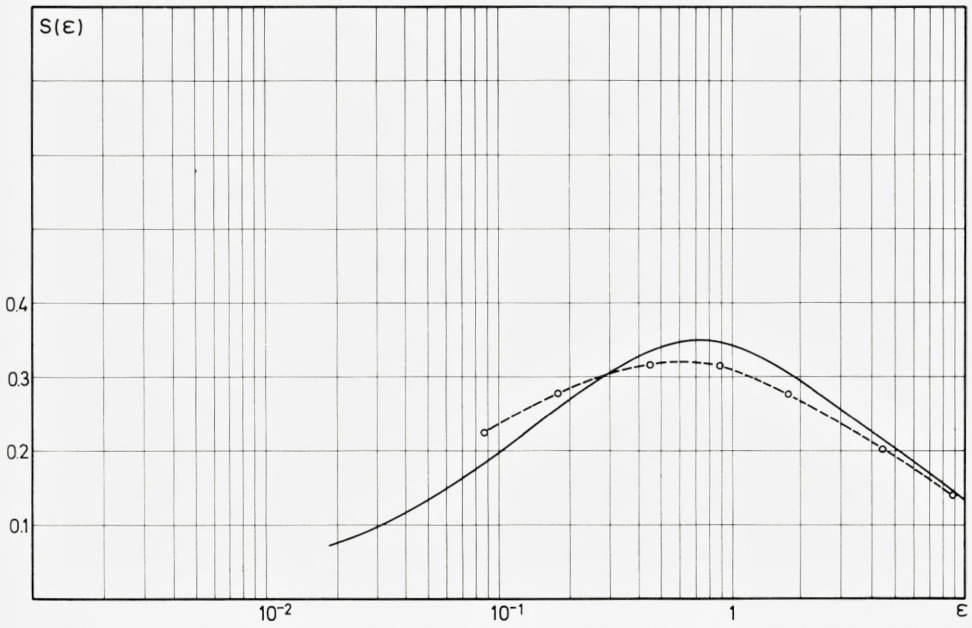

Fig. 9. Reduced stopping cross section $s(\varepsilon)$ for Bohr potential. Comparison between exact calculations (dashed curve), and magic formula (full-drawn curve).

than $\sim 3\,\%$, which is a completely satisfactory agreement in the present connection.

Because of the simplicity of the magic formula and its equivalence to the direct calculations, we use it for a number of comparisons. Thus, in Fig. 6 we compare $f(t^{1/2})$-curves for the Thomas-Fermi, the Lenz-Jensen, and the Bohr potentials. The Bohr potential leads to too low cross sections at low t (i.e. low ε or low θ), and to slightly too high cross sections at $t \sim 1$.

Fig. 7 gives a comparison of the reduced stopping cross section, (4.8), in the three cases represented in Fig. 6. The curves exhibit a similar behaviour as in Fig. 6, with too low stopping cross sections for the Bohr potential at low ε.

Numerical calculations of scattering by simple screened potentials, like the Bohr potential and the Thomas-Fermi potential, have been performed by EVERHART et al.[4], ROBINSON[20], and others. The calculations lead to the differential cross section (2.10), depending on two parameters, ε and $\sin\theta/2$. In Fig. 8 we compare Everhart's calculations of scattering in the Bohr potential with our one-parameter curve. Everhart's curves are shown for

six values of ε; each curve ends at $t^{1/2} = \varepsilon$, corresponding to backward scattering for the ε-value in question. As expected, the deviations from our curve is—in general—largest at backward scattering.

In Fig. 9 is shown the stopping cross section for the Bohr potential, as calculated in the present treatment and from Everhart's cross sections. We may emphasize again that, if it were desirable, one could, e.g., modify the present $f(t^{1/2})$ so as to give the stopping curve of Everhart's calculations (cf. p. 20).

In conclusion, we wish to express our gratitude to many colleagues and friends for their kind interest in the present work. We are particularly grateful to Susann Toldi for patient assistance in the preparation of the paper.

Institute of Physics
University of Aarhus.

References

1) J. Biersack: Reichweiten schwerer Teilchen I: Neutrale Atome in isotroper Bremssubstanz, Hahn-Meitner-Institut für Kernforschung, HMI-B37 (1964).
2) N. Bohr: The Penetration of Atomic Particles through Matter. Mat. Fys. Medd. Dan. Vid. Selsk. **18**, no. 8 (1948).
3) A. Erdélyi, W. Magnus, F. Oberhettinger, and F. G. Tricomi: Higher Transcendental Functions I. McGraw-Hill (1953).
4) E. Everhart, G. Stone, and R. J. Carbone: Classical Calculation of Differential Cross Section for Scattering from a Coulomb Potential with Exponential Screening. Phys. Rev. **99**, 1287 (1955).
5) B. Fastrup, P. Hvelplund, and C. A. Sautter: Stopping Cross Section in Carbon of 0.1–1.0 MeV Atoms with $6 \leq Z_1 \leq 20$. Mat. Fys. Medd. Dan. Vid. Selsk. **35**, no. 10 (1966).
6) O. B. Firsov: Interaction Energy of Atoms for Small Nuclear Separations. Sovj. Phys. JETP **5**, 1192 (1957); Calculation of the Interaction Potentials of Atoms, ibid. **6**, 534 (1958); Scattering of Ions by Atoms, ibid. **7**, 308 (1958).
7) P. Gombás: Die Statistische Theorie des Atoms und ihre Anwendungen. Springer Verlag, Wien (1949); cf. also P. Gombás: Handbuch der Physik, Bd. XXXVI (1956).
8) D. Heinrich: Näherungsmethoden zur Berechnung der klassischen elastischen Streuung zweier Teilchen. Ann. d. Physik, 7. Folge, **13**, 284 (1964).
9) G. Leibfried and T. Plesser: The Convergence Behaviour of Expansions in the Classical Collision Theory. Z. f. Physik **187**, 411 (1965).
10) G. W. Lehmann and K. A. Shapiro: Approximate Analytic Approach to the Classical Scattering Problem. Phys. Rev. **120**, 32 (1960).
11) J. Lindhard and M. Scharff: Energy Dissipation by Ions in the keV Region. Phys. Rev. **124**, 128 (1961).
12) J. Lindhard, M. Scharff, and H. E. Schiøtt: Range Concepts and Heavy Ion Ranges. Mat. Fys. Medd. Dan. Vid. Selsk. **33**, no. 14 (1963).
13) J. Lindhard, V. Nielsen, M. Scharff, and P. V. Thomsen: Integral Equations Governing Radiation Effects. Mat. Fys. Medd. Dan. Vid. Selsk. **33**, no. 10 (1963).
14) J. Lindhard and V. Nielsen: Nuclear Collisions and Ionization Fluctuations in Charged Particle Detectors. Phys. Lett. **2**, 209 (1962).
15) J. Lindhard and P. V. Thomsen: Sharing of Energy Dissipation between Electronic and Atomic Motion. "Radiation Damage in Solids". IAEA, Vienna, Vol. 1, 65 (1962).

16) H. E. Schiøtt: Range-Energy Relations for Low-Energy Ions. Mat. Fys. Medd. Dan. Vid. Selsk. **35**, no. 9 (1966).
17) J. Lindhard: Thomas-Fermi Approach and Similarity in Atomic Collisions. NAS-NRC Publ. 1133, 1 (1964).
18) Ph. Lervig, J. Lindhard, and V. Nielsen: Quantal Treatment of Directional Effects for Energetic Charged Particles in Crystal Lattices. Nucl. Phys. **A 96**, 481 (1967).
19) J. Lindhard: Influence of Crystal Lattice on Motion of Energetic Charged Particles. Mat. Fys. Medd. Dan. Vid. Selsk. **34**, no. 14 (1965).
20) M. T. Robinson: Tables of Classical Scattering Integrals for the Bohr, Born-Meyer, and Thomas-Fermi Potentials. ORNL-3493 (1963).
21) J. W. Sheldon: Use of the Statistical Field Approximation in Molecular Physics. Phys. Rev. **99**, 1291 (1955).
22) P. Sigmund and J. B. Sanders: Spatial Distribution of Energy Deposited by Ion Bombardment. Conf. on Application of Ion Beams to Semiconductor Technology, Grenoble (1967).
23) F. T. Smith, R. P. Marchi, and K. G. Dedrick: Impact Expansions in Classical and Semi-Classical Scattering. Phys. Rev. **150**, 79 (1966).

Indleveret til Selskabet den 20. oktober 1967.
Færdig fra trykkeriet den 8. marts 1968.